Bulletin of Faculty of Science, Zagazig University (BFSZU)))
e-ISSN: 1110-1555
Volume-2024, Issue-2, pp-85-98
https://bfszu.journals.ekb.eg/journal
Research Paper DOI: **10.21608/bfszu.2023.238193.1315**

==========

An overview on structural geophysics application along Cairo-Suez District: Case studies

Kareem Mohsen[1], Mohamed Attwa[1], Ahmed Henaish[1]

[1]Geology Department, Faculty of Science, Zagazig University, Zagazig, 44519, Egypt.
Corresponding author: ahmed_henaish@zu.edu.eg

ABSTRACT **: In recent, it's crucial to thoroughly assess geological conditions and potential hazards when planning and developing urban areas sustainably. Especially in regions where there's limited exposure of rock formations and easily accessible geological data, there's a higher risk of encountering unforeseen hazards. This study tackles this challenge in one of Egypt's heavily deformed areas, offering a comprehensive method for conducting detailed geological and structural mapping in urban settings. This involves collecting data from both the surface and subsurface through field measurements. The aim is to create a detailed profile of the geological conditions, including the underlying structural framework, in a newly established urban hub chosen as a case study. To achieve this, we've carefully mapped out the surface structural data on an intricate geological map, considering the shape and distribution of surface rock layers. We've also conducted a geophysical survey using direct current resistivity (DCR) sounding to reveal the near-surface geology. To overcome the challenges in interpreting DCR sounding data, we've applied both traditional and innovative inversion techniques, making use of available borehole information. Additionally, we've accumulated and analysed the mapped fault segments, both on the surface and in the near-surface, to construct a detailed structural model. Since issues like fault ruptures and the expansion of shale layers have significant implications for sustainable urban development, we've provided an initial assessment of geohazards. This approach offers a comprehensive view of urban geological mapping, providing a foundation for identifying potential hazards or opportunities in the early stages of proposed sustainable development projects.**

KEYWORDS: Urban Geo-Mapping; DCR soundings; Genetic Algorithms; Structural Mapping; Cairo-Suez district.

Date of Submission: 21-09-2023 Date of acceptance: 04-102023

I. INTRODUCTION

With a rapidly growing global population, urban areas are expanding at an unprecedented rate. This surge is notably transforming arid desert lands to meet the escalating demand for urban development, catering to both residential and commercial needs (Elsawy and Lakhouit, 2020). According to a 2019 United Nations report, the world's population is projected to reach a staggering 9.7 billion by the year 2050. Additionally, Sub-Saharan Africa's population is anticipated to double within the same timeframe. Conversely, several regions, including Oceania (excluding Australia/New Zealand), Northern Africa, Western Asia, Australia/New Zealand, Central and Southern Asia, Latin America, the Caribbean, Eastern and Southeastern Asia, and Europe and Northern America, are expected to experience relatively lower population growth rates between 2019 and 2050 (United Nations, 2019).

Given this demographic shift, the study of geological hazards and land resources referred to as urban geology becomes imperative for the expansion and development of new urban areas (El May et al., 2010). In recent years, there has been a growing focus on environmental and urban geology, driven by the need to mitigate urban environmental degradation and the associated geo-environmental hazards that pose threats to burgeoning urban centers (Marker et al., 2003; Cappadonia et al., 2020). In essence, the cornerstones of sustainable development in these new urban areas lie in economical design, stability, and safety.

Geohazards are intricately tied to geological and structural configurations, as well as soil conditions, capable of causing significant damage or even loss of life (Poyiadji et al., 2017). Moreover, a lack of comprehensive data on subsurface geological structures complicates our understanding of subsurface composition, leading to significant geohazards. Thus, establishing databases that encompass all available surface and subsurface information is a crucial requirement to support urban land use planning. As a result, conducting thorough geological and structural assessments in rational urban planning and development can significantly bolster society's resilience to geohazards.

Within the framework of urban geology, structural and geotechnical mapping plays a pivotal role in establishing geotechnical parameters for creating a safe and well-planned urban expansion (Henaish and Attwa, 2018). Additionally, surface geological and structural mapping traditionally rely on literature data, field reconnaissance, and information gathered through field stratigraphic and structural analysis (Sakran et al., 2016; Khalifa et al., 2021). While remote sensing (RS), GIS, and multi-criteria decision analysis have been employed in similar efforts related to urban geology and geo-risk assessment (Lyu et al., 2018; Wang and Li C., 2021), recognizing field geological formations and their tectonic characteristics remains a challenging task. Therefore, integrating RS, GIS, surface geological and structural information, along with subsurface data, is imperative for conducting detailed urban geological and hydrogeological mapping in highly deformed areas (El-Saadawy et al., 2020; Attwa et al., 2020).

As we delve deeper into the subsurface, we encounter a complex interplay of variations and structures that can potentially lead to instability in our urban environments. Traditionally, drilling has been the go-to method for exploring these depths, but it comes at a high cost and consumes a significant amount of time. This is particularly evident in regions where the density of boreholes is low. In contrast, employing in-situ geophysical techniques to gather information about subsurface geology and structures proves to be a non-invasive approach that yields faster results (AkcaandGölebatmaz, 2021; Haydar et al., 2020).

Over time, the failures of numerous urban development projects, coupled with a desire to reduce the reliance on borehole drilling, have prompted the widespread application of geophysical techniques. They're now considered a prerequisite for any successful urbanization endeavor. Integrated geophysical approaches have come to play a pivotal role in the realm of urban geology investigations. These direct ground-based methods enable us to gather physical parameters directly or indirectly linked to lithological and geotechnical characteristics (Perrone et al., 2014). Among these geophysical methods, geoelectrical techniques have seen a surge in applications, ranging from geological and structural studies to landslide and hydrogeological mapping (Lawal et al.,2020; Niculescuand Andrei, 2021; El Bastawesy, 2020) Recently, direct current resistivity (DCR) sounding surveys have proven to be remarkably effective in geological, geotechnical, and hydrogeological assessments (Zhaoet al., 2021). Studies have pointed out that DCR soundings offer a non-destructive means of gathering valid field geological data in arid areas, serving as a cost-effective solution for geological and structural mapping (Attwa and Henaish, 2018; Hagag, 2016).

Taking all of this into consideration, the objective of this case study is to present an integrated approach for mapping urban geology in desert lands. This involves the meticulous collection and analysis of geological, structural, and geophysical data. In this paper, we've specifically employed DCR sounding surveys to obtain meaningful subsurface geological information, complementing and enhancing the existing surface geological and structural data. The fusion of field geophysical data with geological and structural studies allows us to discern the spatial geological characteristics, providing a more comprehensive understanding of geologic hazards, particularly from the perspective of structural geology.

II. REGIONAL GEOLOGY

Geologically, the CSP, depicted in Figure 1, encompasses the northern expanse of the Egyptian Eastern Desert and constitutes a part of an unstable continental shelf. Stretching approximately 120 kilometers, it extends from the bustling city of Cairo in the west to the coastal city of Suez in the east. In terms of tectonics, the CSP has witnessed a series of significant deformation events involving the Arabian, African, and Eurasian plates. These events include: (1) a phase of rifting in the Jurassic-Early Cretaceous period, (2) a transpressive movement in the Late Cretaceous era, and (3) an extension in the Late Oligocene-Early Miocene period, linked to the opening of the Gulf of Suez and continuing into the post-Miocene era. These tectonic occurrences have influenced the distribution of various rock units along the CSP, which encompasses sediments from the Cretaceous, Eocene, Oligocene, Miocene, Pliocene, and Quaternary periods.

From a structural geology perspective, the CSP can be divided into two main sectors, each comprising uplifted blocks and down-faulted sub-basins. The northern province is characterized by faulting and folding affecting Cretaceous, Eocene, Oligocene, and Miocene outcrops (e.g., G. Eweibed; G. Gafra; G. Shabraweet; G. Umm Raqm; G. Hamza; G. Um Qamar) as seen in Figure 1. In contrast, the southern province is marked by distinct Eocene fault blocks and less folded sequences (e.g., G. Ataqa; G. Nasuri; Qattamiya; G. Abu Shama; G. Abu Treifiya SW) also shown in Figure 1. Moreover, the CSP boasts a network of E-W extended fault belts, along with NW-SE trending normal faults, formed by dextral transtension. These faults resulted from the transfer of throw on faults from the Gulf of Suez to the CSP. These fault belts encapsulate various fault geometries and linkage styles as illustrated in Figure1.

Geomorphologically, the CSP spans from the eastern Nile fluvial plain to the western region of the Suez Canal and the northern part of the Gulf of Suez, as indicated inFigure 1. Broadly, the elevation profile of the CSP gradually descends towards the north. The southern part exhibits high elevation and steep slopes, reaching up to 850 meters above mean sea level, as seen in Figure 1, particularly around G. Ataqa to the east. On the contrary, the northern region is predominantly flat, with around 70% of its landmass reaching up to approximately 150 meters above mean sea level, except for localized hilly scarps like G. Eweibed (about 400 meters) and G. Gafra (about 200 meters) shown in Figure 1. The regional slope varies from 0° to 68°, and the average annual precipitation in the study area amounts to around 70 millimeters per year.

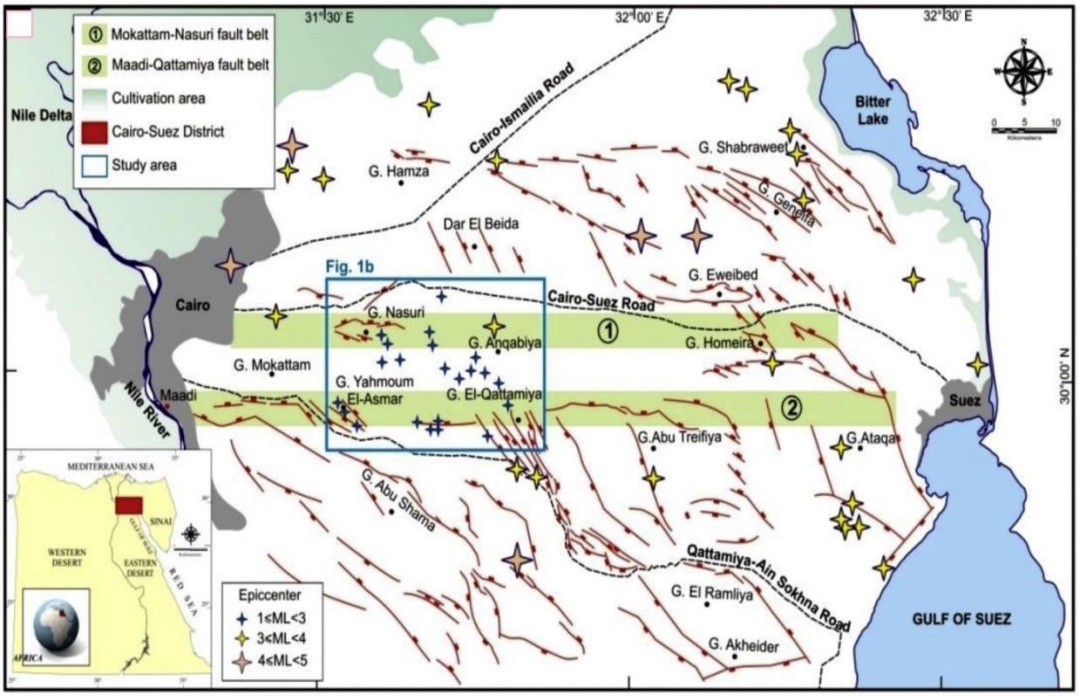

Fig. 1. Shaded relief map (SRTM DEM) with some geological elements: major faults and structural blocks along CSP (compiled from Moustafa&Abd-Allah 1992; Attwa&Henaish, 2018; Henaish&Kharbish, 2020). Note, G: Gebel (mountain).

In a broader sense, the dissected, high-elevated mountains in the southern part are separated by a distinct drainage pattern and interfluves. In contrast, the northern part displays a more widespread dendritic pattern due to its flat and gently sloping topography. Wadi Gafra, highlighted in Figure 1, stands out in the northern region for its dendritic network formed by a master stream and its branches. This network expands in width based on the slope and permeability of the underlying rocks. In the southern CSP, Wadi Ghoweiba, Wadi Hagul, and Wadi El Ramliya (also shown in Figure 1) are the larger extended wadis. It's evident that the main

wadis are structurally influenced, following the paths of major faults, while tributaries are influenced by lithology, fracturing, and regional slope.

The CSP, depicted in Figure 1, encompasses the northern expanse of the Egyptian Eastern Desert and constitutes a part of an unstable continental shelf. Stretching approximately 120 kilometers, it extends from the bustling city of Cairo in the west to the coastal city of Suez in the east. Before delving into the intricacies of structural geology, it was imperative to lay a solid foundation by meticulously documenting the stratigraphy of the region. This involved creating a geological map rooted in the identified formations. The lithostratigraphic information was gathered through extensive fieldwork in the central part of CSD, supplemented by data obtained from borehole observations. Figure 2 encapsulates the range of geological units in the studied area (depicted in Figure 1) spanning from the Middle Eocene epoch to the Recent period.

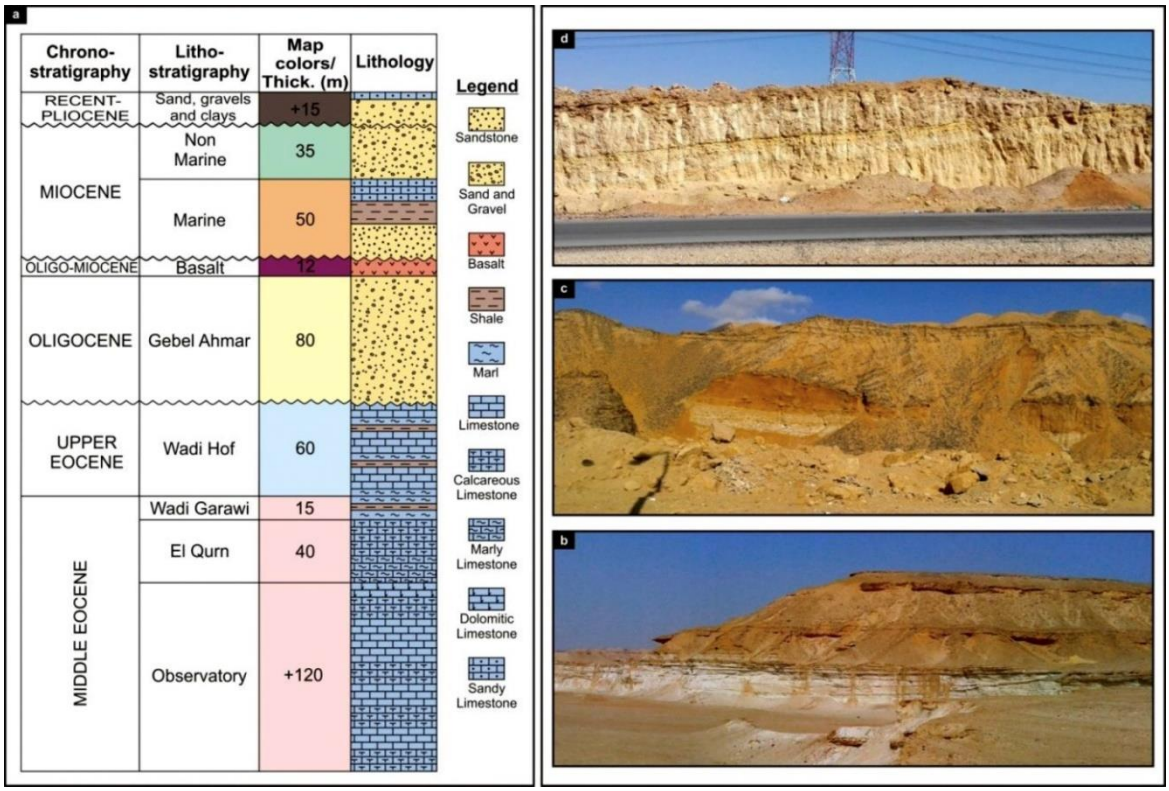

Fig. 2. (a) Composite stratigraphic section of the study area (Attwa and Henaish, 2018). (b) The Upper Eocene sediments at Gebel Yahmoum El-Asmar structural high, looking towards NE. (c) The Oligocene sediments at Gebel El-Qattamiya structural high, looking towards NNE. (d) The Marine Miocene sediments at Gebel Anqabiya structural high, looking towards the SE.

The Middle Eocene period unveils a landscape dominated by limestone and chalky limestone formations known as the Observatory Formation (Farag and Ismail, 1959). This extensive layer surpasses 120 meters in thickness. Overlying it is the El Qurn Formation (Farag and Ismail, 1959), characterized by marly and chalky limestone, reaching an impressive 40-meter thickness. Resting atop the geological canvas is the Wadi Garawi Formation (Farag and Ismail, 1959), a composite of marl and shale, with a breadth of approximately 15 meters. Transitioning to the Upper Eocene rocks (as seen in Fig. 2b), we encounter the Wadi Hof Formation (Farag and Ismail, 1959). This formation, about 60 meters in depth, comprises a medley of shale, marl, and limestone. The Oligocene rocks (Fig. 2c) drape themselves unconformably over the Eocene rocks. Represented by the variegated sands and gravels of the Gebel Ahmar Formation (Shukri, 1954), they amass to roughly 40 meters and find their niche in structural and topographic low points. Additionally, there's the intriguing presence

of basalt flows, dated to the Late Oligocene to Early Miocene era. These flows, appearing in stark contrast, are covered unconformably by the subsequent layers of Miocene and Pliocene rocks. In the realm of the Miocene period, rocks were categorized into two distinctive units, marine and non-marine (Shukri and Akmal, 1953). The marine unit (Fig. 2d) extends to about 50 meters in thickness, composing primarily of sandstone, shale, and sandy limestone. On the flip side, the non-marine unit spans around 35 meters and is characterized by sands and gravels. The Miocene formations bear the weight of the sands, gravels, and sandy limestone from the Pliocene era (Shukri and Akmal, 1953), with thin layers of soil and colluvial sediments blanketing the wadis and scattered areas.

III. STRUCTURAL SETTING

The geological makeup of the Cairo-Suez District (CSD) is a result of intricate tectonic interplay between the African, Eurasian, and Arabian plates (Meshref, 1990). In this specific area (Fig. 1), we find four distinct elevated features: Gebel Nasuri, Gebel Anqabiya, Gebel Yahmoum El-Asmar, and the northern segment of Gebel El-Qattamiya (Fig. 2). These elevated formations are separated by a depression filled with Oligocene rocks (Fig. 1).

Gebel Nasuri stands as an isolated ridge, stretching over 11 kilometers from WNW to ESE, with its highest point reaching an elevation of 345 meters. The exposed rock formations in the Gebel Nasuri fault block primarily belong to the Upper Eocene epoch, except for the easternmost section where Oligocene sands and gravels are prevalent (Fig. 3a and b). Notably, Gebel Nasuri shares its eastern border with Gebel Anqabiya, a landmass mainly comprised of Miocene rocks, spanning an area of approximately 65 square kilometers (Fig. 1). Towards the southwest lies Gebel Yahmoum El-Asmar, reaching up to the Cairo-Ain Sokhna Road (Fig. 1). This feature predominantly showcases Upper Eocene rocks, covering an area of roughly 12 square kilometers, and peaking at an impressive 420 meters in elevation. To the east, Gebel El-Qattamiya (Fig. 2) is characterized mainly by Middle and Upper Eocene rocks. It forms a structural block-oriented NW-SE, with its highest point reaching an elevation of 447 meters. Within our study zone (Fig. 1), we observe a prevailing trend in the bedding dip generally exhibiting a moderate incline towards the northeast. The Eocene rock formations display a gentle to moderate dip, ranging between 10° and 25°, with their orientations influenced by the underlying geological structures. In stark contrast, the Miocene rocks showcase an incredibly subtle dip, rarely exceeding 10°.

From a structural standpoint, the region undergoes deformation primarily through a network of faults and folds, varying in scale. The extensive data amassed during our meticulous field mapping efforts unveils a total of thirty-six documented faults, clustered into four dominant sets, each with a descending frequency – WNW-ESE, NW-SE, ENE-SSW, and NNW-SSE (Fig. 4a and b). Analysis of dip data gathered from five fault surfaces reveals an inclination ranging from moderate to steep, frequently surpassing 65°. Additionally, we have charted nine distinctive folds, falling into two prominent sets, with a descending frequency order – WNW-ESE and NW-SE.

Based on our extensive fieldwork, it becomes evident that folds are prominently displayed across various scales. Notably, at Gebel Nasuri, we encounter the most noteworthy outcrop folds, influencing the Upper Eocene rock formations within this structural high (Fig. 3). Here, we discern two significant anticlines. The first is a double-plunging fold, its axis extending towards the WNW and exerting an impact on the majority of Gebel Nasuri. Conversely, the second fold, situated in the northeastern sector, plunges towards the ENE. Meanwhile, at the far eastern end of Gebel Nasuri, we find the Upper Eocene and Oligocene rocks being influenced by a SW-plunging major syncline (Fig. 3).

Moving on to the central section of Gebel Yahmoum El-Asmar, we come across two gentle, double-plunging anticlinal and synclinal folds, along with an ESE-plunging anticline towards the east. Upon conducting a structural analysis of these folds, it becomes clear that they result from the displacement of beds near the faults, where the fold axes align parallel or sub-parallel to the fault's orientation (Fig. 4a and b). In cases where drag folds are bent, we find synclines within the hanging-wall and anticlines within the footwall (Fig. 4c). Drag

folds emerge as a consequence of lateral and upward fault propagation, often occurring in regions that have been monoclinally flexed at the fault tips. They may also form due to frictional drag along the fault surface, as noted by Schlische in 1995. Notably, drag folds are prominently observed throughout the study area, particularly within the exposed Eocene rocks of Gebel Nasuri and Gebel Yahmoum El-Asmar (Fig. 4d and e).

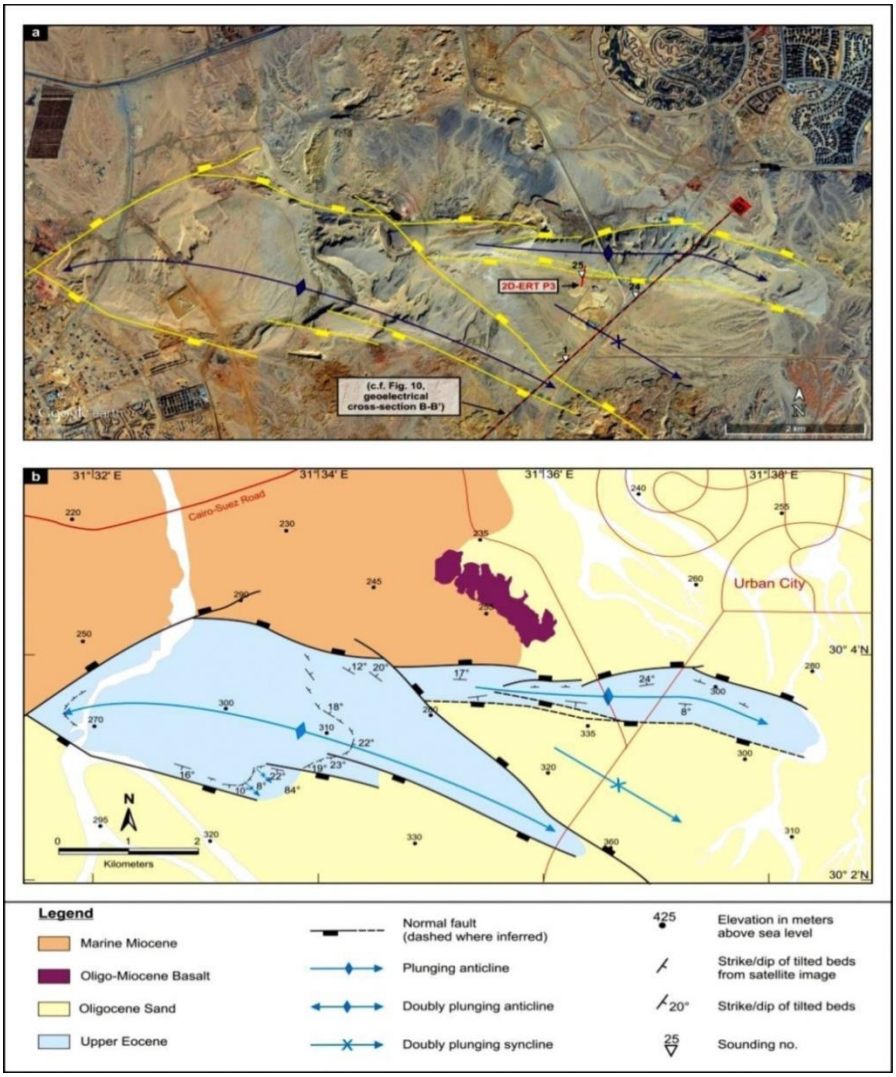

Fig. 3. (a) Google Earth satellite image © 2016 CNES/Astrium and (b) Detailed field geological map of Gebel Nasuri structural high (Attwa and Henaish, 2018).

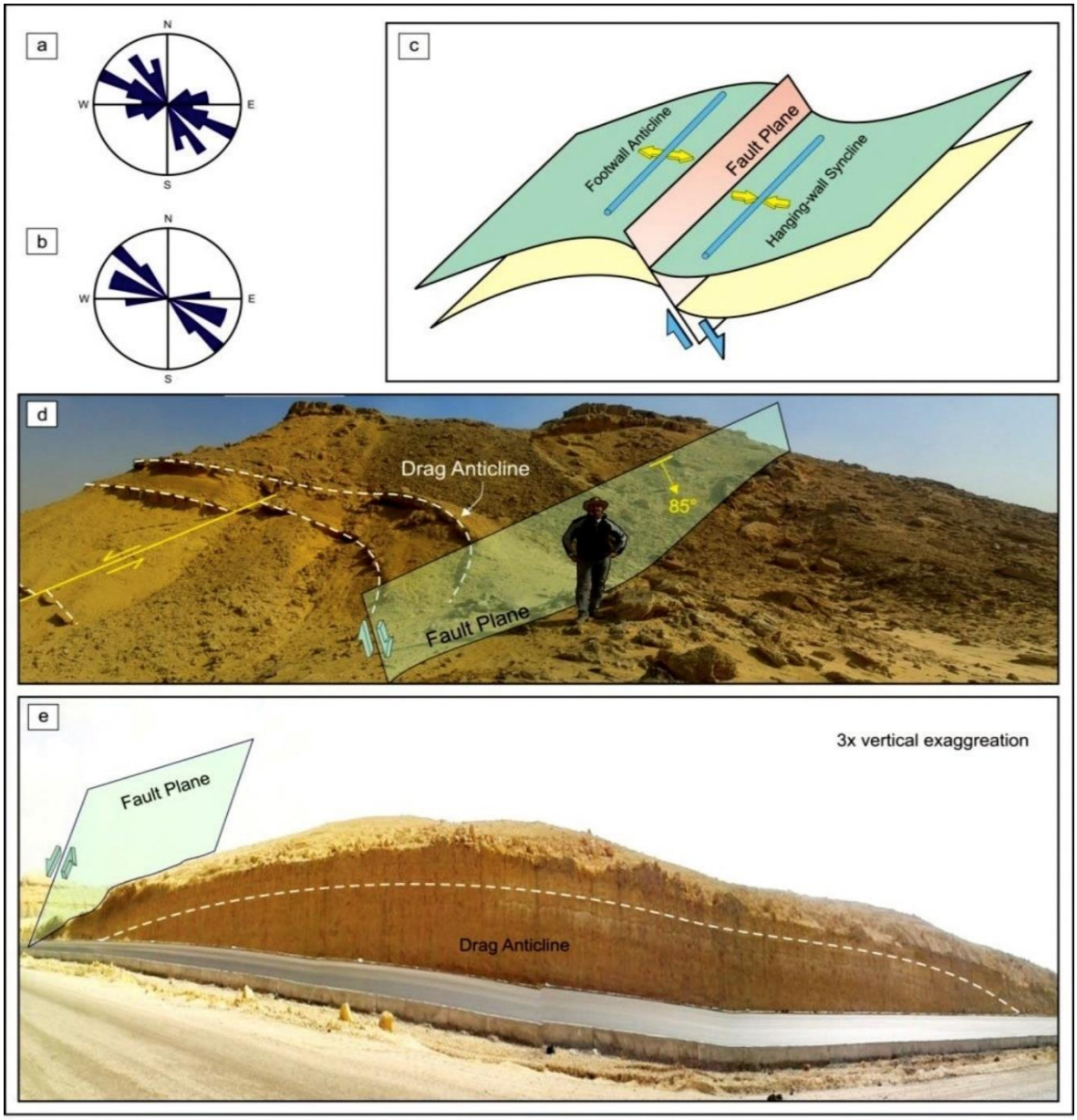

Fig. 4. Strike summary plot showing (a) fault and (b) fold frequency distribution. (c) Schematic model shows the idealized geometry of drag folds. (d) Field photo of an anticlinal drag fold along the footwall of a WNW-ESE normal fault at Gebel Nasuri (looking towards ESE). (e) Field photo of an anticlinal drag fold along the footwall of a WNW-ESE normal fault at Yahmoum El-Asmar (looking towards SE) (Attwa and Henaish, 2018).

IV. METHODOLOGY

Clearly, grasping the geological and structural characteristics of a new urban area is a substantial undertaking, especially when it's situated in desert terrain, before any development takes place. Based on the geological and structural studies previously presented, we can effectively trace and map the tectonic features and geological hazards associated with surface faults and the presence of shale layers. This proactive approach enables us to mitigate geotechnical challenges in areas that are more susceptible to geohazards. Furthermore, Figure-3 serves as a valuable tool for assessing initial engineering ground conditions and other geological-related aspects of surface deposits, offering a representative overview. This discussion helps us understand the practicality and limitations of sustainable development, such as foundation conditions and excavatability, when

reclaiming a new urban area. However, it's important to note that surface geological and structural information must be complemented by subsurface data to construct a comprehensive geometrical structural model that accurately represents bedding plane geometry. To achieve this, we gather borehole and geophysical data, taking into consideration the surface geological and structural findings. This data allows us to create a detailed geological map, which in turn serves as a crucial resource for preliminary urban planning, particularly when dealing with the reclamation of desert lands.

Geophysical Survey

Employing the 1D-DCR technique, we acquired geophysical data, a depth-sounding method widely recognized for constructing accurate geological and structural models in a cost-effective manner (Abotalib et al., 2021; Yilmaz, 2011). In the context of urban geological mapping, the primary objective of these geophysical measurements was to delineate the resistivity distribution of subsurface layers based on surface apparent resistivity readings. Subsequently, the gathered resistivity data were analyzed with respect to subsurface geology and structures, aligning with existing borehole, geological, and structural information (El Bastawesy et al., 2019; Ulem et al., 2021). In essence, the DCR technique involves injecting electrical currents into the subsurface layers through a pair of current electrodes (AB). The resulting fluctuations in electrical potential are then recorded at other pairs of electrodes (MN). This process allows us to measure variations in subsurface resistivity. Within a DCR sounding survey, we can measure apparent resistivity values of subsurface layers at different depths, contingent on the spacing between AB electrodes, in a one-dimensional manner.

Conducting twenty-seven DCR soundings using the conventional Schlumberger array, with a maximum AB spacing of 2000 m (Yilmaz, 2011; Basokur, 1999), revealed that in desert environments, the Schlumberger array proves to be more effective. It provides valuable insights with a favorable signal-to-noise ratio and resolution concerning subsurface characteristics. Considering the geological and structural factors previously discussed, the chosen electrode spacing was determined to be adequate for reaching the necessary depths required for urban geological mapping. We conducted the DCR soundings along as straight survey lines as possible to minimize ambiguity related to ground surface topography. Precise coordinates and elevations for these DCR soundings were obtained using a GPS unit with an accuracy of 2 meters. Furthermore, some of the DCR soundings were strategically positioned near observed boreholes to validate and enhance the accuracy of the DCR interpretation. Given the desert terrain, we conducted the DCR sounding survey with consideration for land accessibility, avoiding hilly areas and quarries. As a result, the distribution of DCR soundings exhibited irregular patterns, and a grid-like arrangement was not feasible.

The DCR soundings were conducted using the SYSCAL Pro resistivity meter (IRIS instrument). Given the arid conditions and relatively high resistance contact of the ground surface in this new urban area reclamation, we utilized stainless steel electrodes surrounded by saltwater and bentonite in a hole to improve poor electrode contact. The ground contact resistance (RS check) was consistently below 5 kΩ. The apparent resistivity data were stacked eight times, and the final data were recorded when the data quality factor values were minimized, with stacked error being less than 2%. Additionally, a standard deviation threshold of below 4% was applied to the data for the interpretation process. Faulty measurements and data with insignificant current or high standard deviation (> 4%) were carefully excluded. Furthermore, apparent resistivity outliers were identified and removed as they indicated poor data quality. We conducted an inversion of the DCR soundings to obtain a multiple-layer model with true resistivities and thicknesses. Leveraging geological information from nearby boreholes, the true resistivities were correlated with the local lithology of the study site. To mitigate uncertainty in the DCR interpretation, we employed both conventional and non-conventional DCR inversion techniques, taking into account borehole information and geological/structural settings.

In the conventional inversion scheme, the DCR soundings underwent an initial inversion process using a sequential interpretation method based on 1D-linear filtering and a damped least-squares algorithm (specifically, the Levenberg-Marquardt method). The sequential method involved an automated iterative approach where initial estimates were refined for layer parameters. The measured resistivity data were smoothed using 1D smoothness weighting schemes, with weight coefficients indicating the likelihood of a perfect fit

(unity) or infinite divergence (zero) between the datasets. Building upon the results of the conventional inversion, we carried out non-conventional inversion using genetic algorithms (GA), which employ heuristic search and select solutions with the lowest misfit values. GA is a flexible technique adaptable to specific problem requirements, and its effectiveness has grown with advancements in computing speed. GA leverages principles from biological evolution, including reproduction, mutation, crossover, and natural selection. In GA, the first generation consists of randomly generated parameter sets representing a conceptual model. Subsequent generations see modifications to parameters through mutation and crossover operations. Models yielding the lowest misfit values, akin to Darwin's theory of survival of the fittest, have a higher likelihood of continuing to the next generation. Ultimately, GA identifies multiple solutions within the global minimum neighborhood. If the global minimum lies within the predefined search space, it can be pinpointed. Consequently, the parameter search space is systematically reduced through successive generations. The final selection of an accurate and specific solution takes into account additional information (e.g., borehole data, geology) and aligns with the interpreter's judgment, considering the nature of the experiment. The ultimate results from each DCR sounding curve provide geoelectrical layers characterized by their resistivity values and thicknesses.

In Figure-5, we present an illustrative interpretation of DCR sounding No. (9). The layer numbers were determined based on insights from borehole data and local geological knowledge. Notably, both the generation numbers and population size were set to 50 (Figure-5a). Within this context, we observe the variation in mean and best misfits against generation (Figure-5a). This plot reveals a rapid decrease in both the smallest and average values, which can be attributed to potential noise in the field data. It's worth noting that the smallest misfit at each generation reaches a limit and cannot be further reduced (i.e., beyond generation 45). Moving on to the best misfit, we observe a commendable alignment between the measured and calculated data (Figure-5b). In further detail, reference (AkçaandBasokur, 2010) elucidates the model response function and error energy map, providing valuable insights into the modeling process. Additionally, robust calibration between borehole information and DCR inversion results, employing genetic algorithms, is evident (Fig. 5c). This underscores the importance of integrating well-established borehole data to accurately delineate subsurface layer distributions. Consequently, this leads to a comprehensive representation of subsurface structures through the constructed geoelectrical cross-sections.

Data Integration

The data gathered from outcrops, along with the analysis conducted, prove to be invaluable when integrated with DCR and borehole data. This integration serves as a crucial control for interpretation, ultimately leading to a more precise urban geological mapping. Utilizing all previously measured structural parameters, we construct a comprehensive integrated structural model. This model sheds light on the necessary precautions to be considered when establishing constructions and infrastructures in close proximity to the mapped faults. These precautions are directly linked to the potential hazards of uncontrolled surface fault ruptures. Consequently, we calculate the minimum setbacks required for both the hanging-walls and footwalls of the mapped faults. This meticulous approach ensures that any urban development in these areas is well-informed and designed to mitigate potential risks associated with fault activity.

V. SUMMARY AND CONCLUSIONS

We applied our proposed approach to uncover the subsurface structural features in a previously unmapped area situated at the central part of CSD (north Eastern Desert, Egypt). This region holds significant potential for urban and industrial expansion, yet it presents a complex structural puzzle tied to the Gulf of Suez rift in Egypt.

In essence, we employed a detailed surface structural benchmark to enhance the precision of interpreting DCR data, reducing any ambiguity. Our journey began with a thorough surface geological mapping effort, which involved a meticulous study of satellite images to identify exposed rock units and outline the primary structural framework. This was followed by fieldwork, where we studied stratigraphic outcrops, measured bedding plane orientations, and documented the geometry of surface geological structures. Subsequently, we conducted trend analysis on the mapped faults and folds to decipher the mechanisms behind structural deformation. We also conducted surface geophysical studies, measuring DCR soundings and Electrical Resistivity Tomography (ERT) data. These results were then integrated to formulate a conceptual subsurface structural model.

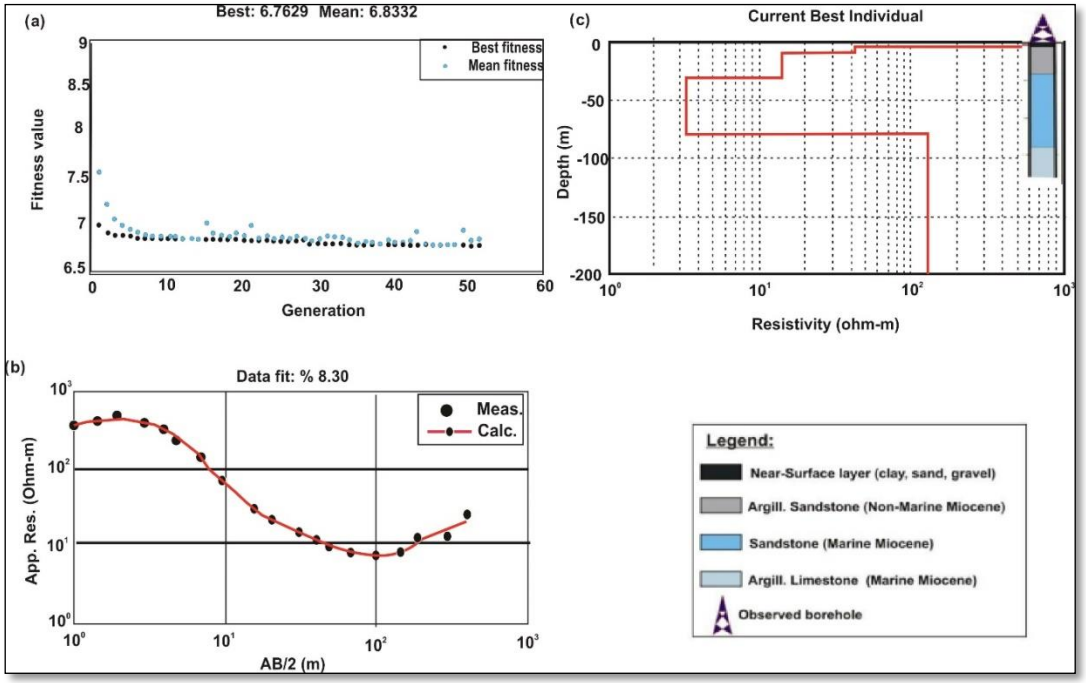

Fig. 5. Interpretation of DCR sounding with borehole data calibration using GA. The population size and generation number were 50. (a) Variation of mean and best misfit versus generation; (b) Acomparison between the measured and theoretical data at the best misfit value; (c) A comparison between the model response resulting from GA and the borehole information (Attwa and Henaish, 2018).

It's important to note that the area's composition as made-ground posed challenges during geophysical data acquisition and interpretation. To overcome this, we sequentially employed derivative-based inversion (DBI) methods and genetic algorithms (GA), which robustified the interpretation process and provided valuable insights for deep and regional geological investigations using DCR soundings. Additionally, we found that prior information from surface structural mapping was crucial to calibrate the inferred regional subsurface structures drawn from the geoelectrical cross-sections.

Further validation was carried out at three selected sites using 2D-ERTs, where the application of L1-norm and an iteratively reweighted algorithm proved instrumental in revealing detailed subsurface structures. These ERTs, in particular, helped unveil intricate details about subsurface geological structures over short distances, which would have been otherwise impossible to discern with 1D data alone or in non-outcropped areas. However, it's worth noting that the presence of highly conductive layers, such as shale, did challenge the resolution and sensitivity of ERTs in identifying subsurface layers. Therefore, we emphasized the importance of

aligning the deduced subsurface structures on 2D-ERTs as closely as possible with known surface features to guide the interpretation.

Ultimately, we projected the deduced structures onto the geological map of the study area, where structural analysis revealed a strong correlation with findings from surface geological mapping. This integrated approach holds significant value for decision-makers, aiding in the planning and assessment of environmental engineering considerations near known structural features. In conclusion, our non-invasive integrated approach serves as a valuable example of how to investigate complex subsurface structures in previously unmapped areas akin to CSD. With further refinement using synthetic models, we hope this approach will continue to improve the ability of ERT to delineate specific complex subsurface structures.

REFERENCES

AbouElenean KM, Mohamed AME, Hussein HM. 2010. Source parameters and ground motion of the Suez-Cairo shear zone earthquakes, Eastern Desert, Egypt. Natural Hazards. 52, 431-451.

Akça I., Basokur AT. 2010. Extraction of structure-based geoelectric models by hybrid genetic algorithms. Geophysics. 75, 15-22.

Akca I., Gölebatmaz SM. 2021. Three-dimensional inversion of DCR data incorporating structural similarity constraint. Journalof Applied Geophysics, 184, 104237. https://doi.org/10.1016/j.jappgeo.2020.104237

Attwa M., El Bastawesy M., Ragab D., Othman A., Assaggaf HM, Abotalib AZ. 2021a. Toward an integrated and sustainable water resources management in structurally-controlled watersheds in desert environments using geophysical and remote sensing methods. Sustainability, 13(7): 4004. https://doi.org/10.3390/su13074004.

Attwa M., El Mahmoudi A., ElshennaweyA.., et al. 2021b. Soil Characterization Using Joint Interpretation of Remote Sensing, Resistivity and Induced Polarization Data along the Coast of the Nile Delta. Natural Resourources Research, 30, 3407-3428. https://doi.org/10.1007/s11053-021-09883-9

Attwa M., El-Shinawi A. 2017. An integrative approach for preliminary environmental engineering investigations amidst reclaiming desert-land: a case study at East Nile Delta, Egypt. Environmental Earth Sciences. 76(8): 304.

Attwa M., Henaish A. 2018. Regional structural mapping using a combined geological and geophysical approach - A preliminary study at Cairo-Suez district, Egypt. Journal of African Earth Sciences, 144, 104-121. https://doi.org/10.1016/j.jafrearsci.2018.04.010

Attwa M., Henaish A., Zamzam S. 2020. Hydrogeologic characterization of a fault-related dome Using outcrop, borehole and electrical resistivity data. Natural Resources Research, 29(2): 1143-1161. https://doi.org/10.1007/s11053-019-09504-6

Basokur AT, Akça I, Siyam NWA. 2007. Hybrid genetic algorithms in view of the evolution theories with application for the electrical sounding method. Geophysical Prospecting. 55, 393-406.

Basokur AT. 1999. Automated 1D interpretation of resistivity soundings by simultaneous use of the direct and iterative methods. Geophysical Prospecting. 47, 149-177.

Batatian D. 2002. Minimum Standards for Surface Fault Rupture Hazard Studies. Salt Lake County Geologic Hazards Ordinance, Appendix A. p. 11.

Cappadonia C., Di Maggio C., Agate M., Agnesi V. 2020 Geomorphology of the urban area of Palermo (Italy). Journal of Maps, 16(2): 274-284. https://doi.org/10.1080/17445647.2020.1739154

Ebong ED, Abong, AA, Ulem EB et al. 2021. Geoelectrical resistivity and geological characterization of hydrostructures for groundwater resource appraisal in the Obudu Plateau, southeastern Nigeria. Natural Resources Research, 30, 2103-2117. https://doi.org/10.1007/s11053- 021-09818-4

El Bastawesy M., Attwa M., Abdel Hafeez TH, Gad A. 2019. Flash floods and groundwater evaluation for the non-gauged dryland catchment using remote sensing, GIS and DC resistivity data: A case study from the Eastern Desert of Egypt. Journal of African Earth Sciences, 152, 245-255. DOI 10.1016/j.jafrearsci.2019.02.004

El Bastawesy M., Gebremichael E., Sultan M., Attwa M., Sahour H. 2020. Tracing Holocene channels and landforms of the Nile Delta through integration of early elevation, geophysical, and sediment core data. The Holocene, 30(8): 1129-1141. doi:10.1177/0959683620913928

El May M., Dlala M., Chenini I. 2010. Urban geological mapping: Geotechnical data analysis for rational development planning, Engineering Geology, 116, 129- 138 https://doi.org/10.1016/j.enggeo.2010.08.002

El-Saadawy O., Gaber A., Othman A., Abotalib AZ, El Bastawesy M., Attwa M. 2020. Modeling flash floods and induced recharge into alluvial aquifers using multitemporal remote sensing and electrical resistivity imaging. Sustainability. 12(23): 10204. https://doi.org/10.3390/su122310204

Elsawy MBD, Lakhouit A. 2020. A review on the impact of salinity on foundation soil of coastal infrastructures and its implications to north of Red Sea coastal constructions. Arabian Journal of Geosciences, 13, 555. https://doi.org/10.1007/s12517-020-05601-6

Fatma K., Yacine D., Haydar B., et al. 2020. Use of electrical resistivity tomography (ERT) and electromagnetic induction (EMI) methods to Characterize Karst Hazards in north-eastern of Algeria. Arabian Journalof Geosciences, 13, 1204. https://doi.org/10.1007/s12517- 020-06206-9.

Gaba`s A., Macau A., Benjumea B., Bellmunt F., Figueras S., Vila M. 2014. Combination of Geophysical Methods to Support Urban Geological Mapping. Surveys inGeophysics, 35, 983-1002. DOI 10.1007/s10712-013- 9248-9

Goldberg DE. 1989. Genetic Algorithms in Search, Optimization and Machine Learning. Addison-Wesley, Boston, Mass.

Gouasmia, M., Khorchani, H., Mhamdi A., et al. 2018. Hydrogeological characterization of a carbonateaquifer using geophysical and geochemical approach: case of the Krachoua Formation in Tataouine area, Southern Tunisia. Arabian Journal of Geosciences, 11, 786. https://doi.org/10.1007/s12517-018-4150-x

Guiraud R., Bosworth W. 1997. Senonian basin inversion and rejuvenation of rifting in Africa and Arabia: synthesis and implications to plate-scale tectonics. Tectonophysics. 282, 39-82.

Guiraud R., Bosworth W. 1999. Phanerozoic geodynamic evolution of northeastern Africa and the northwestern Arabian platform. Tectonophysics. 315, 73-108.

Hagag W. 2016. Structural evolution and Cenozoic tectonostratigraphy of the Cairo-Suez district, north Eastern Desert of Egypt: Field-structural data from Gebel Qattamiya-Gebel Um Reheiat area. Journal of African Earth Sciences. 118, 174-191.

Henaish A. (2018b). Fault-related domes: Insights from sedimentary outcrops at the northern tip of the Gulf of Suez rift, Egypt. Marine and Petroleum Geology, 91, 202- 210. https://doi.org/10.1016/j.marpetgeo.2018.01.009

Henaish A. 2018a. Soft-linkage transfer zones: Insights from the Northern Eastern Desert, Egypt. Marine and Petroleum Geology, 95, 265-275.https://doi.org/10.1016/j.marpetgeo.2018.05.005

Henaish A., Attwa M. 2018. Internal structural architecture of a soft-linkage transfer zone using outcrop and DC resistivity data: Implications for preliminary engineering assessment. Engineering Geology, 244: 1-13. https://doi.org/10.1016/j.enggeo.2018.07.018

Henaish A., Kharbish S. 2020. Linkage style of riftassociated fault arrays: insights from central Cairo-Suez district, Egypt. Carpathian Journal of Earth and Environmental Sciences, February 2020, 15(1): 189-196.

International Code Council. 2000. International building code. International Code Council. p. 297.

Issawi B., Sallam ES, Salem M. 2018. Tectonostratigraphic and sedimentary evolution of the Ubur-Orabi sub-basin, southeast Nile Delta, Egypt. Carbonates and Evaporites, 33, 663-681. https://doi.org/10.1007/s13146-017-0392-z

Khalifa A., Bashir B., Çakir Z., Kaya Ş., Alsalman A., Henaish A. 2021. Paradigm of Geological Mapping of the Adıyaman Fault Zone of Eastern Turkey Using Landsat 8 Remotely Sensed Data Coupled with PCA, ICA, and MNFA Techniques. ISPRS International Journal of Geo-Information, 10(6): 368. https://doi.org/10.3390/ijgi10060368

Kharbish S., Henaish A. and Zamzam S. Geodiversity and geotourism in Greater Cairo area, Egypt: implications for geoheritage revival and sustainable development. Arabian Journal of Geosciences, 13, 451. https://doi.org/10.1007/s12517-020-05457-w

Lawal A., Tijani MN, D'Alessio M. 2020. Geoelectrical characterisation of aquifers in Bauchi-Alkaleri-Kirfi geological transition zones, Northeast Nigeria. Environmental Earth Sciences, 79, 224. https://doi.org/10.1007/s12665-020-08978-5 Lyu H-M, Shen JS, Arulrajah A. 2018. Assessment of Geohazards and Preventative Countermeasures Using AHP Incorporated with GIS in Lanzhou, China. Sustainability. 10(2): 304. https://doi.org/10.3390/su10020304

Marker BR, Pereira JJ, de Mulder EEJ. 2003. Integrating Geological Information into Urban Planning and Management: Approaches for the 21st Century. Earth Science in the City: A Reader, p 379. https://doi.org/10.1029/SP056p0379

Meshref WM. 1990. Tectonic framework of Egypt. In: Said R, ed. The geology of Egypt. Balkema, Rotterdam, Netherlands, 133-155.

Moustafa AR, Abd-Allah MA. 1991. Structural setting of the central part of the Cairo-Suez District. Middle East Research Center, Ain Shams University, Earth Science Series. 5, 133-145.

Moustafa AR, Abd-Allah MA. 1992. Transfer zones with en echelon faulting at the northern end of the Suez rift. Tectonics. 11, 499-509.

Moustafa AR, El Badrawy R., Gibali H. 1998. Pervasive E-ENE oriented faults in northern Egypt and their effect on the development and inversion of prolific sedimentary basins. In: 14th E.G.P.C. Petrol. Conf. Cairo. 1, 51-67.

Moustafa AR, Yehia MA, Abdel Tawab S. 1985. Structural setting of the area east of Cairo, Maadi, and Helwan. Middle East Research Center, Ain Shams University, Earth Science Series. 5, 40-64

Moustafa AR. 2002. Controls on the geometry of transfer zones in the Suez rift and northwest Red Sea: Implications for the structural geometry of rift systems. AAPG Bulletin. 86, 979-1002.

Niculescu BM, Andrei G. 2021. Application of electrical resistivity tomography for imaging seawater intrusion in a coastal aquifer. ActaGeophysica, 69, 613-630. https://doi.org/10.1007/s11600-020-00529-7

Perrone A., Lapenna V., Piscitelli S. 2014. Electrical resistivity tomography technique for landslide investigation: A review. Earth-Science Reviews, 135, 65- 82. https://doi.org/10.1016/j.earscirev.2014.04.002.

Poyiadji E., Kontogianni V., Nikolaou N. 2017. Integration of geohazards in urban planning and management. Advanced Engineering Forum, ISSN: 2234- 991X 21:557-563. https://doi.org/10.4028/www.scientific.net/AEF.21.557

Saad A. 2013. Geological, Soil and Rock Mass Evaluation for Risk Assessment of Badr City, Egypt. Middle East Journal of Applied Sciences. 3(4): 265-276.

Sakran S.M., Nabih M., Henaish A., Ziko A. O. 2016. Fracture reopening by micro-earthquakes, a mechanism for oil seepage in mildly active rifts: a Case study from Gemsa oil field, the southern Gulf of Suez rift, Egypt. Arabian Journal of Geosciences. 9(5): 1-17.

Shukri NM, Akmal MG. 1953. The geology of Gebel El Nasuri and Gebel El-Anqabiya district. Bulletin de la Société de géographied'Egypte. 26, 243-276.

Sun L, Liu Q., Grasselli G., Tang X. 2020. Simulation of thermal cracking in anisotropic shale formations using the combined finite-discrete element method. Computers and Geotechnics. 117, 103237.

United Nations. 2019. The Sustainable Development Goals Report, p 61. https://doi.org/10.18356/55eb9109-en

Wang H., Li C. 2021. Analysis of scale effect and change characteristics of ecological landscape pattern in urban waters. Arabian Journal of Geosciences, 14, 569. https://doi.org/10.1007/s12517-021-06831-y Alkaradaghi K., Ali SS, Al-Ansari N., Laue J., Chabuk A. 2019. Landfill site selection Using MCDM methods and GIS in the Sulaimaniyah Governorate, Iraq. Sustainability, 11(17): 4530. https://doi.org/10.3390/su11174530

Yilmaz S. 2011. A case study of the application of electrical resistivity imaging for investigation of a landslide along highway. International Journal of Physical Sciences, 6(24): 5843-5849. DOI: 10.5897/IJPS11.564

Zhao Y., Yu Y., Yang H., et al. 2021. Vertical electric soundings characteristics of paleochannel in the Yuyao River Valley, Eastern China. Bulletin of Engineering Geology and the Environment, 80, 1047-1061. https://doi.org/10.1007/s10064-020-01951-3